



Research papers

Multi-model projections of future evaporation in a sub-tropical lake



Sofia La Fuente^{a,*}, Eleanor Jennings^a, Gideon Gal^b, Georgiy Kirillin^c, Tom Shatwell^d, Robert Ladwig^e, Tadhg Moore^f, Raoul-Marie Couture^g, Marianne Côté^g, C. Love Råman Vinnå^h, R. Iestyn Woolwayⁱ

^a Centre for Freshwater and Environmental Studies, Dundalk Institute of Technology, Dundalk, Ireland

^b Kinneret Limnological Laboratory, Israel Oceanographic & Limnological Research, Migdal, Israel

^c Leibniz-Institute of Freshwater Ecology and Inland Fisheries (IGB), Berlin, Germany

^d Helmholtz Centre for Environmental Research, Department of Lake Research, Magdeburg, Germany

^e Center for Limnology, University of Wisconsin-Madison, Madison, WI, USA

^f Virginia Tech, Department of Biological Sciences, Blacksburg, VA, USA

^g Centre for Northern Studies (CEN), Takuvik Joint International Laboratory, and Department of Chemistry, Université Laval, Quebec City, QC, Canada

^h Eawag, Swiss Federal Institute of Aquatic Science and Technology, Surface Waters - Research and Management, Kastanienbaum, Switzerland

ⁱ School of Ocean Sciences, Bangor University, Menai Bridge, Anglesey, Wales

ARTICLE INFO

This manuscript was handled by Marco Borga, Editor-in-Chief, with the assistance of Lixin Wang, Associate Editor

Keywords:

Ensemble modelling
Lake evaporation
Climate change
Lake Kinneret

ABSTRACT

Lake evaporation plays an important role in the water budget of lakes. Predicting lake evaporation responses to climate change is thus of paramount importance for the planning of mitigation and adaptation strategies. However, most studies that have simulated climate change impacts on lake evaporation have typically utilised a single mechanistic model. Whilst such studies have merit, projected changes in lake evaporation from any single lake model can be considered uncertain. To better understand evaporation responses to climate change, a multi-model approach (i.e., where a range of projections are considered), is desirable. In this study, we present such multi-model analysis, where five lake models forced by four different climate model projections are used to simulate historic and future change (1901–2099) in lake evaporation. Our investigation, which focuses on sub-tropical Lake Kinneret (Israel), suggested considerable differences in simulated evaporation rates among the models, with the annual average evaporation rates varying between 1232 mm year⁻¹ and 2608 mm year⁻¹ during the historic period (1901–2005). We explored these differences by comparing the models with reference evaporation rates estimated using in-situ data (2000–2005) and a bulk aerodynamic algorithm. We found that the model ensemble generally captured the intra-annual variability in reference evaporation rates, and compared well at seasonal timescales (RMSEc = 0.19, R = 0.92). Using the model ensemble, we then projected future change in evaporation rates under three different Representative Concentration Pathway (RCP) scenarios: RCP 2.6, 6.0 and 8.5. Our projections indicated that, by the end of the 21st century (2070–2099), annual average evaporation rates would increase in Lake Kinneret by 9–22 % under RCPs 2.6–8.5. When compared with projected regional declines in precipitation, our projections suggested that the water balance of Lake Kinneret could experience a deficit of 14–40 % this century. We anticipate this substantial projected deficit combined with a considerable growth in population expected for this region could have considerable negative impacts on water availability and would consequently increase regional water stress.

1. Introduction

Lake evaporation plays a fundamental role in the basic functioning of lakes. Evaporation directly and, in some cases, substantially modifies the hydrologic, chemical, and energy budgets, making it one of the most

important physical controls on lake ecosystems (Schindler, 2001; Lenters et al., 2005; Riveros-Iregui et al., 2017; Woolway et al., 2020). Not only does lake evaporation play a fundamental role in these budgets through the physical removal of fresh water, but the cooling effect of latent heat flux is also central to the modification of lake temperature,

* Corresponding author at: Centre for Freshwater and Environmental Studies, Dundalk Institute of Technology, Dundalk, Marshes Upper A91 K584, Co. Louth, Ireland.

E-mail address: ruthsofia.lafuentepillco@dkit.ie (S. La Fuente).

<https://doi.org/10.1016/j.jhydrol.2022.128729>

Received 9 June 2022; Received in revised form 5 October 2022; Accepted 11 October 2022

Available online 9 November 2022

0022-1694/© 2022 The Author(s). Published by Elsevier B.V. This is an open access article under the CC BY license (<http://creativecommons.org/licenses/by/4.0/>).

and related processes such as stratification (Mishra et al., 2011; Lenters et al., 2013; Spence et al., 2013; Van Cleave et al., 2014) and vertical mixing (MacIntyre et al., 2009; Ye et al., 2019), with likely impacts on lake chemistry and biota (Likens et al., 2009; Williamson et al., 2009; Wahed et al., 2014). Importantly, lake evaporation also contributes to critical feedbacks within lakes, including interactions between evaporation and lake surface temperature (Lenters et al., 2013; Spence et al., 2013; Van Cleave et al., 2014; Ye et al., 2019; Kishcha et al., 2021), feedbacks between salinity and evaporation rates (Shilo et al., 2015; Riveros-Iregui et al., 2017), and the coupling of evaporation with changes in lake level and extent (Marsh and Bigras, 1988; Li et al., 2013; Friedrich et al., 2018; Zhan et al., 2019). While evaporation substantially influences various processes within the lake, fluctuations in water level represent, arguably, one of the most important ones for the ecosystem services that lakes provide. A decline in lake water level can have major implications for access to clean water, collection of food via fishing, the transportation of goods, energy generation, and ecosystem loss (Zohary and Ostrovsky, 2011).

Evaporation in lakes is largely governed by the magnitude of the vapor pressure gradient between the lake surface and the overlying atmosphere (Hostetler and Bartlein, 1990; Lenters et al., 2005, 2014). This gradient, and thereafter the transfer of latent heat, is determined primarily by the temperature of the lake surface, the absolute humidity in the atmosphere, and the amount of wind-induced turbulent mixing at the air–water interface (Lenters et al., 2014; Woolway et al., 2018). Some of the most direct atmospheric drivers of lake evaporation are thus wind speed and absolute humidity i.e., the basis of eddy covariance measurements. However, due to the influence of lake surface temperature on the vapor pressure gradient, other atmospheric and limnological factors which influence the lake heat budget also play a considerable role in evaporation (Brutsaert, 1982; Lenters et al., 2005; Friedrich et al., 2018). Overall, the sources of available energy that influence lake evaporation are numerous, including incoming radiation (both solar and longwave), sensible heat flux (via changes in the Bowen ratio), advected heat (snowfall, groundwater, etc.), and changes in heat stored within the lake itself. The energy available for evaporation is also modulated by the amount of outgoing longwave and shortwave radiation, which are dictated by lake surface temperature and shortwave albedo, respectively. In addition to these climatic drivers, numerous lake-specific features, such as water clarity, wind sheltering and lake depth, can modify the timing and/or intensity of lake evaporation, primarily through influences on lake surface temperature, heat storage, and wind mixing (McVicar et al., 2012; Read et al., 2012; Zhan et al., 2019). As a result of these complex interactions and the dependence of many lake-specific factors, evaporation is highly variable between lakes (Marsh and Bigras, 1988; Woolway et al., 2018; Wang et al., 2018; Konapala et al., 2020; Zhou et al., 2021).

Given the significance of lake evaporation, as well as its complex interactions with other within-lake processes, predicting its response to climate change is of paramount importance. To accurately simulate lake evaporation responses to historic and future climatic variations, process-based numerical models that can compute complex air–water and within-lake thermodynamic fluxes are needed. A number of such process-based models have been developed in recent decades, including those based on, among other things, eddy-diffusion (Hostetler and Bartlein, 1990; Hostetler et al., 1993), bulk formulation (Mironov, 2008), energy balance (Hipsey et al., 2019), and turbulence closure (Burchard et al., 1999; Goudsmit et al., 2002). However, most studies that simulate climate change impacts on lake evaporation have utilised only a single mechanistic model (Hostetler and Bartlein, 1990; Vallet-Coulomb et al., 2001; Lenters et al., 2005; Wang et al., 2018). Whilst such studies have merit, most lake models implement approximate forms of relationships, either due to incomplete knowledge of some processes or for practical computing purposes. Furthermore, any individual model provides an approximation of reality, for which uncertainty is often not quantified (Moore et al., 2021). An alternate method is

to adopt an ensemble approach, where multiple, independently developed models are used. Such coordinated experiments have become the *de facto* standard in climate science including, for example, the Coupled Model Intercomparison Project (Meehl et al., 2005). Ensemble modelling of lake responses to climate change is, however, in its infancy (Trolle et al., 2014; Gal et al., 2020; Mesman et al., 2020; Grant et al., 2021; Moore et al., 2021; Woolway et al., 2021; Feldbauer et al., 2022).

The overarching aim of this study was to investigate changes in lake evaporation under historic and future climate using a suite of independently developed lake models forced with projections from multiple General Circulation Models (GCMs) to produce an ensemble of lake-climate model projections. Our study was focused on Lake Kinneret (Israel), a lake with high socio-economic, political, and religious value. Also known as the Sea of Galilee, Lake Kinneret provides ~ 25–30 % of the drinking water in Israel (Shilo et al., 2015) and ~ 100 million m³ year⁻¹ to the Kingdom of Jordan. Analysing the impacts of climate change on evaporation rates in Lake Kinneret is thus of primary importance for adaptation and mitigation strategies. Here, we investigate (i) multi-model projections of lake evaporation during the historical period and evaluate key differences across the model ensemble; (ii) assess the accuracy of the model ensemble relative to a reference evaporation estimated using observed data at seasonal, annual and intra-annual timescales; and (iii) using the model ensemble, we investigate future projections of lake evaporation this century under different climate change scenarios.

2. Methods and materials

2.1. Study area

Lake Kinneret is a sub-tropical monomictic lake located in the northern region of Israel (Fig. 1). The average surface area of the lake is 168.7 km² with an average volume of 4100 Mm³ (Zohary et al., 2014). The mean and maximum depths of Lake Kinneret are 25.6 and 41.7 m, respectively (Shilo et al., 2015), and its average residence time is ~ 8–10 years (Rimmer et al., 2009; Van Emmerik et al., 2013). Climatic conditions in the region can be categorised as warm and dry, with annual average air temperatures of ~ 21 °C (maximum > 36 °C), annual average rainfall of 380 mm year⁻¹, and surface winds often exceeding ~ 10 m s⁻¹ (Zohary et al., 2014; Gal et al., 2020). The main inflows of Lake Kinneret are the Jordan and Meshushim rivers, and considerable water input comes as runoff and from saline springs as groundwater. The most

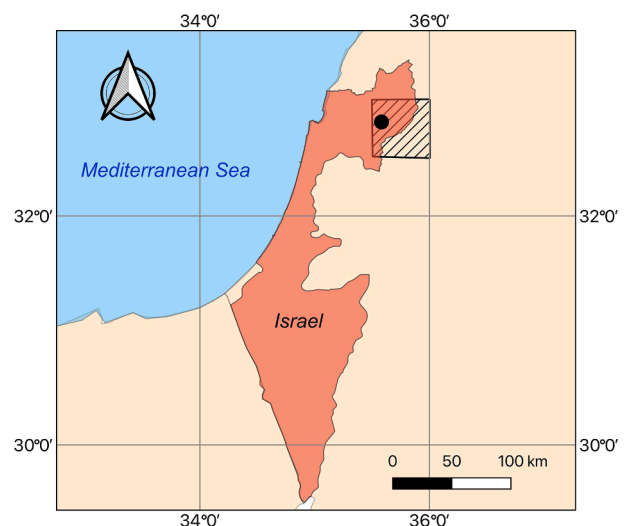


Fig. 1. Map of Israel with the location of Lake Kinneret shown by the filled black circle. The shaded region represents the spatial domain of the ISIMIP2b input data used to drive the lake models.

important outflows from the lake consist of water withdrawals via the National Water Carrier (NWC), the Degania dam and pumping around the lake by local consumers (Gal et al., 2003).

2.2. Multi-model projections of lake evaporation

Lake projections investigated in this study were a lake-climate model ensemble of 20 model realizations. More specifically, from five lake models driven by four GCMs. The lake models, namely FLake (Mironov, 2008), GLM (Hipsey et al., 2019), GOTM (Burchard et al., 1999), MyLake (Saloranta and Andersen, 2007), and Simstrat (Goudsmit et al., 2002) (Table 1), contributed to the Inter-Sectoral Impact Model Inter-comparison Project (ISIMIP) phase 2b Lake Sector (Golub et al., 2022). A description of each lake model used is provided below.

2.2.1. Lake models description

FLake is a 1-D bulk model based on a two-layer parametric representation of the evolving temperature profile and on the integral budgets of heat and kinetic energy for the layers in question. The structure of the stratified layer between the upper mixed layer and the basin bottom is described using the concept of self-similarity (assumed shape) of the temperature-depth curve (Kirillin, 2002). The same concept is used to describe the temperature structure of the thermally active upper layer of bottom sediments and, when present, of the ice and snow cover (Mironov, 2008). FLake uses a lake-specific parameterization scheme to compute the fluxes of momentum, and of sensible and latent heat flux at the lake surface based on the Monin-Obukhov similarity relations.

GLM (General Lake Model) (Hipsey et al., 2019) is a process-based 1-

D hydrodynamic model that provides lake volume-averaged output over the vertical axis. It applies the integral energy assumption to calculate mixed layer depth from external turbulent kinetic energy. Mixing below the mixed layer depth is calculated through a parameterization of the eddy diffusivity coefficient to local gradients of buoyancy and shear. GLM applies a flexible grid structure, which allows the model grid cells to vary in thickness and total number of cells during a simulation. The latent heat flux in GLM is calculated using the algorithm presented in Imberger and Patterson (1981).

GOTM (General Ocean Turbulence Model) (Burchard et al., 1999) is a vertical 1-D hydrodynamic water column model that includes key processes related to vertical mixing in marine and fresh waters (Umlauf and Lemmin, 2005). It has been adapted for use in hydrodynamic modelling of inland water bodies (Sachse et al., 2014). GOTM is often used as a stand-alone model for investigating boundary layer dynamics in natural waters, but it can also be coupled to biogeochemical models. The surface fluxes of momentum, sensible and latent heat are calculated according to the bulk formulae explained by Fairall et al. (1996). This model has been used to model CO₂ dissolution (Enstad et al., 2008), water quality in lakes (Kong et al., 2022), to predict lake ecosystem state (Andersen et al., 2020) and to hindcast the thermal structure of lakes (Ayala et al., 2020; Moras et al., 2019).

MyLake is a 1-D process-based model used to simulate physical, chemical and biological dynamics in lakes (Saloranta and Andersen, 2007). The model simulates thermal stratification, lake ice and snow cover, and phytoplankton dynamics, along with sediment-water interactions using a simple sediment box model (v.1.12). MyLake uses regularly spaced water layers whose vertical resolution is defined by the

Table 1

Summary of the lake models used in this study, including a description of their structure, parameterization and key references.

Lake model (version)	Timestep Simulated/ Reported	Vertical structure / layers reported	Parameterization of turbulent fluxes at air-water interface	Turbulent mixing parameterization	Calibrated parameters	Key references
FLake (ver. 2.0)	Daily	Two-layer self-similar structure / 4	The Monin-Obukhov similarity relations	The water surface temperature is equal to the mixed-layer temperature, this is computed from calculation and constant update of heat fluxes	1. Parameter for profile relaxation time	Mironov (2008)
GLM (ver. 3.0.0)	Daily	Multilayer / 0.5 m - max. depth	Algorithm used in Imberger and Patterson (1981)	Energy balance approach for surface layer mixing, eddy diffusivity approach for deep mixing	1. Diffuse attenuation coefficient 2. Longwave (or cloud) scaling factor 3. Wind speed scaling factor	Hipsey et al. (2019)
GOTM (ver. 5.1)	Daily	Multiple / 0.5 m - max.depth	Based on Fairall et al. (1996)	k-ε model	1. e-folding depth for visible; and e-folding depth for non-visible fraction of light 2. Minimum turbulent kinetic energy 3. Surface heat-flux factor 4. Shortwave radiation factor 5. Wind factor	Umlauf and Lemmin (2005); Burchard et al. (2006)
MyLake (ver. 1.12)	Daily	Multilayer / 0.5 m - max. depth	Diffusion coefficient in heat balance	Hondzo and Stefan thermal diffusion model	1. Wind shelter parameter 2. Minimum stability frequency 3. Non-PAR diffuse attenuation coefficient 4. PAR diffuse attenuation coefficient	Saloranta and Andersen (2007)
Simstrat (ver. 2.1.2)	Daily	Multilayer / 0.5 m - max depth	Dirichlet condition	k-ε turbulence model with buoyancy and internal seiche parameterization	1. Fraction of wind energy transferred to seiche energy 2. As above during summer and winter 3. Fraction of forcing wind to wind at 10 m 4. Fit parameter scaling absorption of IR radiation from sky	Goudsmit et al. (2002)

user. The turbulent fluxes at the air-water interface are estimated using a diffusion coefficient in the heat balance as explained by Hondzo and Stefan (1993). Different versions of the model have been developed to simulate algal blooms (Salk et al., 2022), CO₂ and CH₄ (Kiuru et al., 2019), internal phosphorus loads (Markelov et al., 2019) and light attenuation dynamics (Pilla and Couture, 2021).

Simstrat is a physical deterministic 1-D hydrodynamic model, including vertical mixing induced by internal seiches and surface ice (Goudsmit et al., 2002; Gaudard et al., 2019). This model uses layers of fixed depth (at 0.5 m intervals for lakes with < 50 m maximum depth and at 1 m intervals for lakes > 50 m), and supports multiple options for external forcing, comprising several meteorological variables or surface energy fluxes. Simstrat simulates thermal stratification and ice and snow formation (Gaudard et al., 2019). The surface fluxes are calculated using the Livingstone and Imboden (1989) formulae. Simstrat has been applied in lakes of varying climatic and morphometric conditions (Thiery et al., 2014; Kobler and Schmid, 2019; Mesman et al., 2020; Råman Vinnå et al., 2021; Bärenbold et al., 2022).

2.2.2. Input data and calibration

Bias-adjusted climate projections from the Coupled Model Inter-comparison Project (CMIP5) (Lange, 2019) were used to drive each lake model in a one-way direction (i.e. lake-to-atmosphere interactions were not considered). Specifically, the lake models were driven by four GCMs: GFDL-ESM2M, HadGEM2-ES, IPSL-CM5A-LR, and MIROC5 during the 20th and 21st century (1901–2099). Historic simulations were forced using anthropogenic greenhouse gas and aerosol forcings in addition to natural forcing, and covered the period 1901 to 2005. Future projections simulate the evolution of the climate system under three different greenhouse gas emission scenarios Representative Concentration Pathways (RCP): RCP 2.6 (low-emission scenario), RCP 6.0 (medium-high-emission scenario), and RCP 8.5 (high-emission scenario), over the period 2006 to 2099. These pathways encompass a range of potential future global radiative forcing from anthropogenic greenhouse gases and aerosols. The climate data used to drive each lake model included projections of air temperature at 2 m, wind speed at 10 m, surface downwelling shortwave and longwave radiation, precipitation and specific humidity (Table 2). The climate data had a spatial resolution of 0.5° and covered the whole lake surface (Fig. 1). Additional input data to the lake models included the hypsographic relationship between depth and surface area (i.e. lake bathymetry), and water transparency (Golub et al., 2022). Salinity feedbacks, water inputs and withdrawals were not considered in the ISIMIP2b simulations. The calibration of the lake models in ISIMIP2b consisted of parameters and coefficients related to processes controlling surface heat and energy fluxes, light attenuation and turbulent kinetic energy and wind (Table 1). In addition, different optimization functions were used to minimize the difference between simulated and measured water temperatures. Specific details of model calibration and optimization are given by Golub et al. (2022).

Lake models in ISIMIP2b simulated historic and future projections of

lake physical properties including, among other things, daily simulations of lake surface water temperature and latent heat flux. These data were used in this study to estimate evaporation rates in Lake Kinneret as:

$$E = \frac{Q_e}{\rho_o L_v} \quad (1)$$

where E is evaporation rate (m s^{-1}), Q_e is the latent heat flux (W m^{-2}), ρ_o is density of surface water (kg m^{-3}), calculated as a function of surface water temperature, T_0 ($^{\circ}\text{C}$), and $L_v = 2.501 \times 10^6 - 2370T_0$ is the latent heat of vaporization (J kg^{-1}) (Henderson-Sellers, 1986).

2.3. Validation of simulated evaporation rates

We compared our simulations of lake evaporation from Lake Kinneret with those estimated from observed data (2000–2005), hereafter referred to as the reference evaporation. Most notably, meteorological data measured on the lake surface, and the algorithms available within the LakeMetabolizer package in R (Woolway et al., 2015; Winslow et al., 2016), were used to estimate the latent heat flux over the observational period, and subsequently the evaporation rates (Eq. (1)), using the bulk aerodynamic algorithm of Zeng et al. (1998). The motivation to use the algorithm of Zeng et al. (1998), as opposed to the many others available (Fairall et al., 2003; Verburg and Antenucci, 2010), is that this bulk transfer method has been described as one of the least problematic bulk aerodynamic algorithms used by the scientific community for estimating surface energy fluxes (Brunke et al., 2003) and due to the open-access tools available for its calculation (Woolway et al., 2015; Winslow et al., 2016). In brief, this algorithm applies the Monin-Obukhov similarity theory to the atmospheric boundary layer and states that wind, temperature and humidity profile gradients depend on unique functions of the stability parameter (Text S1).

The latent heat flux, Q_e , used to estimate the reference evaporation was calculated as:

$$Q_e = \rho_z C_{ez} u_z (q_0 - q_z) \quad (2)$$

where $\rho_z = 100p/[R_a(T_z + 273.16)]$ is the density of the overlying air (kg m^{-3}); p is the surface air pressure (hPa); $R_a = 287(1 + 0.608q_z)$ is the gas constant for moist air ($\text{J kg}^{-1} \text{ } ^{\circ}\text{C}^{-1}$); u_z is the wind speed (m s^{-1}) at height z_u (7.8 m) above the water surface; T_z is air temperature ($^{\circ}\text{C}$) at height z_t (6.3 m) above the water surface; $q_0 = \lambda e_{sat}/p$ is the specific humidity at saturation pressure in kg kg^{-1} , with λ representing the ratio of the molecular weights for dry and moist air; e_{sat} is the saturated vapour pressure (hPa), calculated as $e_{sat} = 6.11 \exp\left[\frac{17.27T_0}{237.3+T_0}\right]$; where T_0 ($^{\circ}\text{C}$) is water surface temperature; $q_z = \lambda e/p$ is the specific humidity of the air (kg kg^{-1}) at height z_q (6.3 m) above the water surface, where $e = R_h e_z/100$ is actual vapour pressure, R_h is the relative humidity (%) and $e_z = 6.11 \exp\left[\frac{17.27T_z}{237.3+T_z}\right]$ is the saturated vapour pressure (hPa) at z_t . Here,

Table 2

Climate forcing variables used as input to drive the lake models used in this study to simulate historical and future evaporation rates in Lake Kinneret.

Variable	Abbreviation	FLake	GLM	GOTM	MyLake	Simstrat
Near-surface relative humidity [%]	hurs		x		x	
Near-surface specific humidity [kg kg^{-1}]	huss	x		x		x
Precipitation [$\text{kg m}^{-2} \text{ s}^{-1}$]	pr		x	x	x	x
Surface pressure [Pa]	ps			x	x	x
Surface downwelling longwave radiation [W m^{-2}]	rlds	x	x			x
Surface downwelling shortwave radiation [W m^{-2}]	rsds	x	x	x	x	x
Near-surface wind speed at 10 m [m s^{-1}]	sfWind	x	x	x	x	x
Near-surface air temperature [K]	tas	x	x	x	x	x
Eastward near-surface wind [m s^{-1}] (*)	uas			x		x
Northward near-surface wind [m s^{-1}] (*)	vas			x		x

(*) Not included in the bias-correction.

C_{ez} is the transfer coefficient for height z_q , which was calculated after correcting for wind measurement height and atmospheric stability (Zeng et al., 1998) (Fig. S1). Using the estimated daily C_{ez} , we calculated an average C_{ez} of 1.7×10^{-3} during the study period, which is comparable to those estimated in other lakes (Table S1). A detailed description of the estimation of reference evaporation is provided in the supplementary material (Text S1). The calculated Q_e was then used to estimate E using Eq. (1). The estimated reference evaporation was also validated with monthly evaporation from water-solute-heat balances available from the Israel National Water Supply Company (Mekorot) over the common period 2000–2005.

Meteorological data over the 2000–2005 period was collected at a fixed height on-lake weather station (Tabgha) located in the northwest region of Lake Kinneret ~ 1 km offshore from the Kinneret Limnological Laboratory (35.54° longitude and 32.86° latitude). Air temperature and relative humidity were measured using a Young temperature/relative-humidity sensor probe model 43372C at 6.3 m above water surface. Shortwave radiation (305–2800 nm; $W m^{-2}$) and downwelling long-wave radiation (5–25 nm; $W m^{-2}$) were measured using a Kipp & Zonen Delft BV pyranometer CM11 and CG1, respectively at 6.5 m above water surface. Wind speed and direction were measured using a Young wind monitor MA-05106 at 7.8 m above the water surface. Water surface temperature was measured by a Young platinum floating temperature probe model 41,342 at a depth of ~ 0.05 m (Gal et al., 2003; Rimmer et al., 2009). The reported measurement error of the water temperature observations was ± 0.005 °C (Rimmer et al., 2009; Van Emmerik et al., 2013). The sample frequency at the Tabgha station was 10 min, and maintenance works were carried out once a month. Precipitation observations were collected from an on-shore weather station located ~ 2 km from the southern point of the lake.

2.4. Statistical methods

To assess the performance of the lake model simulations, we compared reference and simulated evaporation rates over the common period (2000–2005), by estimating the normalized Mean Bias Error (MBE) and the normalized Root Mean Squared Error (RMSEC), and then summarizing the results within a Target Diagram (Jolliff et al., 2009). In addition, the Spearman Rank correlation (R) was used to assess the ability of the models to reproduce seasonal and intra-annual variability patterns from the reference evaporation.

2.5. Historic and future projections of precipitation and population

Complementary to our lake evaporation projections, we used historic and future projections of precipitation (P) in the region. These were also available from ISIMIP2b (Frieler et al., 2017). Projections of P and E were used in this study to estimate changes to the net flux of water between the atmosphere and the surface ($P - E$) during the historic and future periods. This net flux was also used to provide insights into potential future changes to the volume of water in Lake Kinneret. The precipitation data consisted of daily values for historic and future scenarios available for the four GCMs and the three RCPs used in projecting future changes in lake evaporation. In addition, we obtained historic and future population projections for the study area that were available from the ISIMIP3b for two Shared Socio-economic Pathways (i.e. SSP-1 comparable to RCP 2.6, and SSP-5 comparable to RCP 8.5) at a 0.5-degree spatial resolution. For Lake Kinneret and the surrounding region, we defined a bounding box of longitude: 34.25° – 36° and latitude: 29.25° – 33.75° when extracting the gridded population data. Concurrent changes in the local population and $P - E$ are used here to provide insights into changes in water stress within the region in the future. Precipitation and population data are freely available from the ISIMIP data repository at <https://data.isimip.org>.

3. Results

3.1. Validation of simulated evaporation rates

We compared simulated evaporation rates from our lake-climate model ensemble with the reference evaporation over the period 2000–2005. Our analysis suggests that lake evaporation estimates were sensitive to the choice of lake model. At daily and seasonal timescales, the reference evaporation was generally within the range of those simulated by the model ensemble, which suggests that they adequately capture the intra-annual variability of the reference evaporation. Moreover, the mean of the model ensemble followed closely the seasonal variation in the reference evaporation (Fig. 2). To better assess the performance of the individual lakes models, we compared the monthly reference and simulated evaporation rates with three performance metrics, namely the Spearman Rank Correlation (R), RMSEC, and MBE (Fig. 3; Table 3). Our analysis suggested that, among the lake models tested, MyLake compared best with the reference evaporation ($R = 0.88$; $RMSEC = 0.14$; $MBE = -0.04$), followed by FLake ($R = 0.77$; $RMSEC = 0.19$; $MBE = -0.05$), GOTM ($R = 0.86$; $RMSEC = 0.23$; $MBE = 0.18$), Simstrat ($R = 0.76$; $RMSEC = 0.31$; $MBE = 0.27$) and GLM ($R = 0.77$; $RMSEC = 0.43$; $MBE = 0.41$). Furthermore, a high correlation and low error ($R = 0.92$; $RMSEC = 0.19$; $MBE = 0.15$) was calculated between the mean of the lake-climate model ensemble and the reference evaporation (Fig. 4a). Overall, our comparison suggests that the mean of the models performed better than most of the individual models, and considerably better than the worst performing model (Fig. 4). Although, it is important to note that the mean of the ensemble showed slightly higher evaporation rates relative to the reference evaporation, particularly when evaporation rates were low (Fig. 4a). Moreover, a comparison of reference and simulated evaporation rates at seasonal timescales suggested that some models (e.g., FLake and MyLake) generally underestimated the reference evaporation rates during all seasons except winter, while the opposite was true for other models (e.g., GOTM, GLM and Simstrat), which overestimated evaporation rates in all seasons (Table 4). We also calculated the percent error in simulated seasonal evaporation rates, which demonstrated considerable variability in the performance of lake models across seasons. For instance, the models with the lowest percent error across seasons were MyLake (–17 % to 21 %) and FLake (–24 % to 43 %). GOTM exhibited errors between 5 % and 45 %, followed by Simstrat (20 % and 99 %), and GLM (38 % and 111 %) (Table 4). Overall, our results suggest that for this particular lake, and during the time period of interest, one could argue that MyLake and FLake performed best when simulating the reference evaporation. However, this could be due to the positive and negative seasonal biases of these lake models being compensated for, and thus resulting in an overall lower bias than GOTM, GLM and Simstrat. Most impressive was the performance of the model ensemble, and particularly the mean, in capturing the seasonality in reference evaporation rates. Importantly, our analysis suggests that some lake models perform better than others during some parts of the year, and that including information from the ensemble is desirable. Finally, a comparison revealed that the reference evaporation closely captured the intra-annual variability of Mekorot evaporation estimates, which is reflected by the high correlation and low error estimated ($R = 0.91$; $RMSEC = 0.10$; $MBE = -0.02$) (see Fig. 2a and Fig. S2), suggesting that our reference evaporation is robust and can be used as a basis for validation of our simulations.

3.2. Multi-model projections of lake evaporation during the 20th and 21st century

Following the validation of our model ensemble from 2000 to 2005, we investigated long-term historic and future changes in evaporation rates over the period 1900–2099. Specifically, we investigated differences across the lake-climate model ensemble in order to evaluate any discrepancies in projected future change (Fig. 5). The future projections

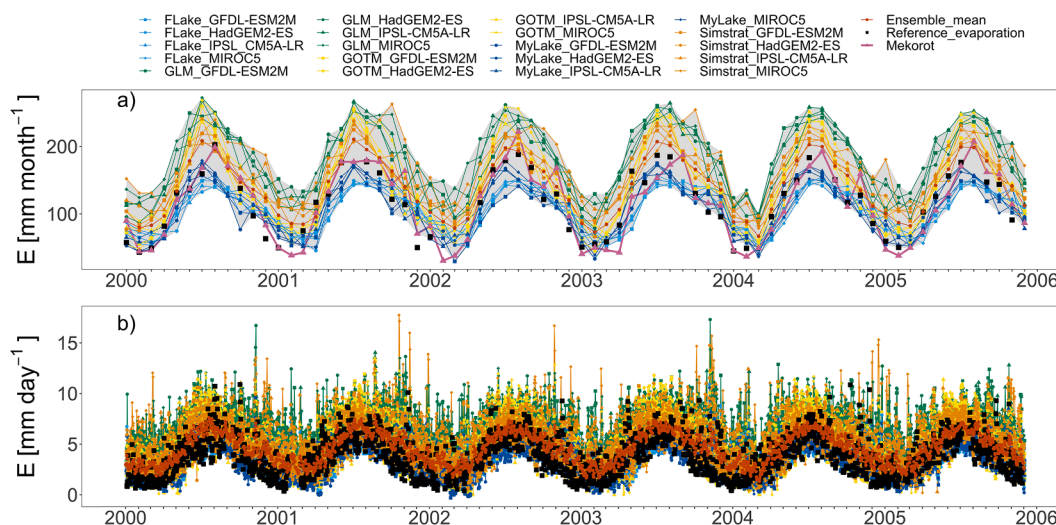


Fig. 2. Simulated and reference evaporation rates over the historic period (2000–2005) in Lake Kinneret shown at (a) monthly and, (b) daily timescales. Each coloured line represents simulations from a unique lake model forced by an ensemble of GCMs. Pink lines in panel a represent the Mekorot evaporation rates (only available at monthly time steps). Orange lines represent the average of simulated lake evaporation rates from the lake-climate model ensemble. The shaded region in panel a represents the spread (min and max) across the model ensemble. (For interpretation of the references to colour in this figure legend, the reader is referred to the web version of this article.)

showed noticeable differences in lake evaporation anomalies (i.e., the difference between lake evaporation in a given time period relative to the base period [1971–2000] average) across the model ensemble. By the end of this century (2070–2099), our results indicate that, for the high-emissions scenario (RCP 8.5), MyLake and FLake projected the smallest increase in evaporation rates of 320 mm year⁻¹ and 329 mm year⁻¹, respectively, whereas GOTM (452 mm year⁻¹), GLM (438 mm year⁻¹) and Simstrat (388 mm year⁻¹) projected the highest change in evaporation rates (Table 5). Similar results were found during the historical period where the highest evaporation rates were estimated by GLM, GOTM and Simstrat. Furthermore, our analysis suggests that the magnitude of projected change in evaporation rates differ considerably depending on the GCM used to drive the lake models. Particularly, the average end of century evaporation anomalies across the GCMs (i.e. averaged across all lake models) varied between 109 mm year⁻¹ (GFDL-ESM2M) and 227 mm year⁻¹ (HadGEM2-ES) under RCP 2.6, between 220 mm year⁻¹ (GFDL-ESM2M) and 323 mm year⁻¹ (HadGEM2-ES) under RCP 6.0, and between 334 mm year⁻¹ (GFDL-ESM2M) and 441 mm year⁻¹ (HadGEM2-ES) under RCP 8.5. Thus, the lake simulations using GFDL-ESM2M as input data projected considerably lower evaporation rates this century, and those using HadGEM2-ES projected the greatest change, on average.

Given the differences in simulated evaporation rates among the lake-climate model ensemble, it seems relevant to combine the individual ensemble members and to calculate the average and standard deviation among them. The model ensemble indicated an average annual evaporation of 1784 ± 473 mm year⁻¹ (quoted uncertainties represent the standard deviation from the model ensemble) during the latter stages of the 20th century (1971–2000 average). During the 21st century (2006 to 2099), the average of the model ensemble demonstrates that evaporation rates are projected to increase considerably in Lake Kinneret (Fig. 6). Under RCP 2.6, lake evaporation is projected to increase by 160 ± 70 mm year⁻¹ by the end of the 21st century (2070 to 2099). For RCP 6.0, lake evaporation is projected to increase by 258 ± 76 mm year⁻¹. The largest change in lake evaporation is projected under RCP 8.5 with evaporation rates increasing by 385 ± 93 mm year⁻¹. These projected changes correspond to a percent increase of 9 %, 14 % and 22 %, for RCP 2.6, 6.0 and 8.5 respectively, compared to the base-period average (Table 6).

The magnitude of change in lake evaporation will not be the same throughout the year, but will change differently across seasons (Fig. 7).

Moreover, similar to our projections of annual evaporation rates, the projected changes in evaporation across seasons will vary across the lake-climate model ensemble. Our future projections of seasonal evaporation show an overall increase compared to the historic period for all seasons and RCP scenarios (Fig. 7; Table 7). In the historic period (1971–2000) evaporation estimates were between 314 ± 77 mm season⁻¹ in the winter and 621 ± 197 mm season⁻¹ in the summer. We calculated the projected changes in seasonal evaporation by the end of the 21st century (2070–2099) and found that the greatest change occurred in spring, corresponding to an increase of 12 % for RCP 2.6, 20 % for RCP 6.0 and 30 % for RCP 8.5. These changes were followed by an increase in evaporation during autumn, corresponding to an increase of 9 % for RCP 2.6, 14 % for RCP 6.0 and 20 % for RCP 8.5 (Table 7). The lowest changes across RCP scenarios were detected in the winter with increases of 8 %, 10 % and 19 % under RCPs 2.6, 6.0 and 8.5 respectively.

3.3. Concurrent changes in precipitation and evaporation

To evaluate the potential impact of the simulated changes in lake evaporation on water level in Lake Kinneret, we analysed the combined impacts of climate change on precipitation and evaporation at annual timescales. Changes in precipitation for our study site were highly variable, with an overall decreasing trend from 2005 until the end of the 21st century for all RCPs (Fig. 8a). The average precipitation over the historic period was 454 ± 100 mm year⁻¹, but decreased by -28 ± 109 mm year⁻¹ (-6%), -98 ± 117 mm year⁻¹ (-22%), and -145 ± 102 mm year⁻¹ (-32%) by the end of the century under RCP 2.6, 6.0 and 8.5, respectively (Table 8). By calculating the difference between precipitation and evaporation (P-E), our analysis showed that the change in multi-model average evaporation was projected to be greater than the change in multi-model average precipitation. These results suggest that changes in lake evaporation will likely be greater than those in precipitation under all RCPs this century. Notably, all RCPs suggested a decrease in P-E until the end of the century (Fig. 8b). This change reflected the rapid increase in projected evaporation rates and the concurrent substantial decrease in projected precipitation this century within the study region. Relative to the 1971–2000 base period average (-1330 ± 488 mm year⁻¹), P-E continuously decreased throughout the 21st century. Notably, under RCPs 2.6, 6.0 and 8.5, P-E will decrease by -188 ± 129 mm year⁻¹, -356 ± 148 mm year⁻¹, and -530 ± 145 mm

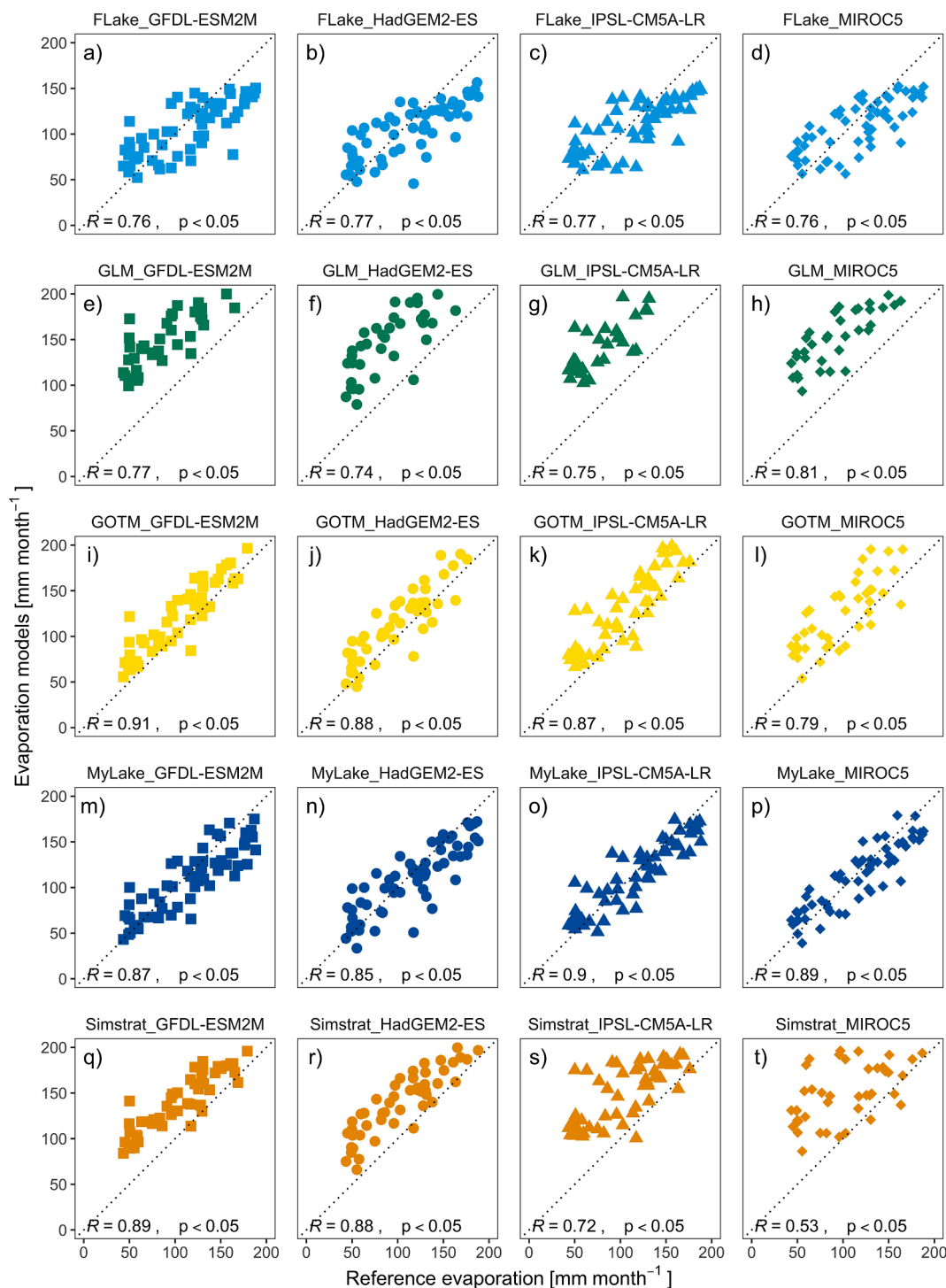


Fig. 3. Monthly averaged simulated and reference evaporation rates from 2000 to 2005. Evaporation rates are compared with the Spearman Rank correlation (R), which is shown in the bottom left of each panel. The dashed line represents the 1:1 relationship between simulated and reference evaporation rates. Results are shown for each combination of lake climate models, namely (a-d) FLake, (e-h) GLM, (i-l) GOTM, (m-p) MyLake and (q-t) Simstrat, driven by the four General Circulation Models included in this study.

year⁻¹, respectively, by the end of the 21st century (2070–2099) (Fig. 8b). These changes represent a percent change in P-E of -14 %, -27 % and -40 % under RCP 2.6, 6.0, and 8.5, respectively (Table 8).

The local population within the study region, which was estimated to be around 10 million people during the 1971–2000 base period, is projected to increase during the twenty-first century (Fig. 8b). Projections for the shared socioeconomic pathways SSP-1 and SSP-5 (i.e. comparable to RCP 2.6 and RCP 8.5, respectively) showed a pronounced

future increase compared to the historical period. In the case of SSP-1/RCP 2.6 there was a steep increase projected for the local population until the mid-21st century (i.e., 2050 s), and afterwards a more steady increase towards 2099, with an average population of 33 million. Under SSP-5/RCP 8.5, the future projections demonstrate a very steep increase of population starting from 2005, with an average population of 42 million people by the end of this century. When comparing these increases to the historical period, we estimated a striking increase in

Table 3
Summary of Spearman rank correlation values (R), the Root Mean Square Error (RMSEc) and the Mean Bias Error (MBE) for lake-climate models with respect to reference evaporation over the period 2000–2005.

Lake model	Driving GCM	Spearman rank correlation [R]	RMSEc	MBE
FLake	GFDL-ESM2M	0.76	0.19	-0.05
FLake	HadGEM2-ES	0.77	0.20	-0.06
FLake	IPSL-CM5A-LR	0.77	0.19	-0.04
FLake	MIROC5	0.76	0.19	-0.05
GLM	GFDL-ESM2M	0.77	0.43	0.41
GLM	HadGEM2-ES	0.74	0.42	0.40
GLM	IPSL-CM5A-LR	0.75	0.45	0.43
GLM	MIROC5	0.81	0.44	0.42
GOTM	GFDL-ESM2M	0.91	0.19	0.14
GOTM	HadGEM2-ES	0.88	0.21	0.14
GOTM	IPSL-CM5A-LR	0.87	0.23	0.18
GOTM	MIROC5	0.79	0.30	0.24
MyLake	GFDL-ESM2M	0.87	0.15	-0.05
MyLake	HadGEM2-ES	0.85	0.16	-0.04
MyLake	IPSL-CM5A-LR	0.90	0.13	-0.02
MyLake	MIROC5	0.89	0.13	-0.03
Simstrat	GFDL-ESM2M	0.89	0.25	0.23
Simstrat	HadGEM2-ES	0.88	0.26	0.23
Simstrat	IPSL-CM5A-LR	0.72	0.32	0.28
Simstrat	MIROC5	0.53	0.41	0.34
Ensemble mean		0.92	0.19	0.15

population of 248 % for the RCP 2.6 scenario, and 337 % for the RCP 8.5 (Table 8).

4. Discussion

Projecting future changes in lake evaporation is critical for ecosystem and water resource management, particularly in areas where these resources are already under immense pressure (Givati et al., 2019; Prange et al., 2020). In this study, we provide an assessment of projected changes in evaporation rates in Lake Kinneret, a socioeconomically important lake in the Middle East, using a model ensemble of 20 lake-

climate model combinations (5 lake models and 4 GCMs). We found that the ensemble mean of the models tested was superior to most of the individual lake-climate model realizations in describing the reference evaporation rates in Lake Kinneret during the historical period. This is in agreement with our expectations and in-line with experiences on the use of ensemble modelling within the climate science community (Trolle et al., 2014; Moore et al., 2021), which have often shown that an ensemble approach provides more robust projections of complex systems compared to any single model. By applying 20 lake-climate model combinations to simulate one lake, we were able to understand key differences in model performance and, likewise, to demonstrate the usefulness of an ensemble approach for projecting lake responses to climate change. The lake-climate models generally agreed on the seasonal variability in evaporation rates, and match those shown in the reference evaporation calculated using observational data, with the ensemble mean often showing the best performance. Regarding our future projections, our analysis also demonstrated that it is critical to consider an ensemble of both lake and climate model simulations when projecting future change in lakes, given the spread of the projected changes.

Although we believe that this study bridges an important knowledge gap, there are some limitations that should be considered when interpreting our findings. Firstly, our projections are generated with 1-D process-based lake models, and thus horizontal features in lakes and the intra-lake responses to climate change will not be captured (Laval et al., 2003). In practice, the 1-D lake models used in this study assume that evaporation rates are uniform over the entire lake surface given that input data to the models was available for one location representative of the lake. However, field observations in different regions have shown that the spatial distribution of lake evaporation is highly variable (Mahrer and Assouline, 1993; Lenters et al., 2013). Similarly, one might expect within-lake differences in the magnitude of change in lake evaporation rates under climate change, as has already been demonstrated for lake surface temperature (Mason et al., 2016; Woolway and Merchant, 2018). The intra-lake variability in evaporation rates could be simulated with 3-D lake models, but these complex models are data intensive and computationally expensive (Amadori et al., 2021), and therefore are not often used for ensemble lake modelling, particularly for investigating future change (Zamani et al., 2021). Furthermore, our comparison of the simulations with reference evaporation from Lake

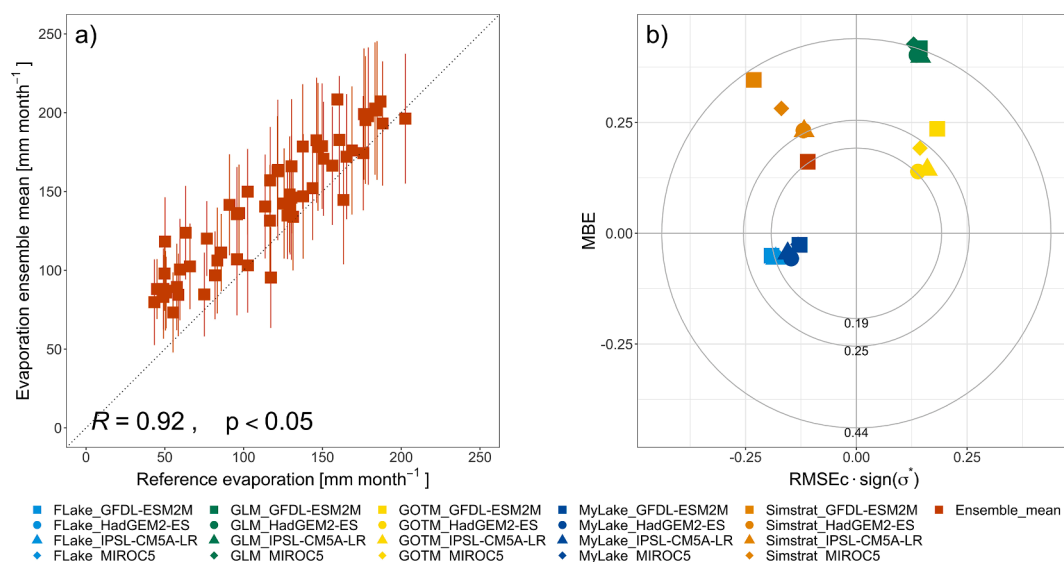


Fig. 4. Shown are (a) a comparison of reference evaporation rates with the average projections across the lake-climate model ensemble (2000–2005); and (b) a target diagram which summarizes the normalized Mean Bias Error (MBE) and the normalized Root Mean Squared Error (RMSEc) of all simulated evaporation rates across the lake-climate model ensemble. The error bars surrounding the ensemble mean represent the standard deviation of the model ensemble over the 2000–2005 period. The dashed line in panel a represents the 1:1 relationship between the reference evaporation and the ensemble mean.

Table 4

Comparison of seasonal evaporation rates between the lake models and the reference evaporation over the period 2000–2005. The colour code indicates when the lake model overestimates (blue) and underestimates (red) the reference evaporation. Darker/lighter colours indicate a higher/lower overestimation/underestimation of models.

Lake model	Driving GCM	Seasonal evaporation [mm season ⁻¹]				Error [%]			
		Summer (JJA)	Autumn (SON)	Winter (DJF)	Spring (MAM)	Summer (JJA)	Autumn (SON)	Winter (DJF)	Spring (MAM)
FLake	GFDL-ESM2M	420	384	259	217	-19	-4	42	-27
FLake	HadGEM2-ES	413	373	259	222	-20	-6	42	-25
FLake	IPSL-CM5A-LR	416	389	263	230	-20	-2	45	-22
FLake	MIROC5	412	396	260	229	-20	-1	43	-23
GLM	GFDL-ESM2M	703	609	397	433	36	53	118	46
GLM	HadGEM2-ES	717	605	382	442	39	52	110	49
GLM	IPSL-CM5A-LR	726	616	380	462	41	55	109	56
GLM	MIROC5	712	622	380	456	38	56	109	54
GOTM	GFDL-ESM2M	639	450	253	299	24	13	39	1
GOTM	HadGEM2-ES	673	435	243	313	30	9	33	6
GOTM	IPSL-CM5A-LR	669	467	277	317	29	17	52	7
GOTM	MIROC5	696	539	285	313	35	35	57	6
MyLake	GFDL-ESM2M	456	357	218	238	-12	-10	20	-20
MyLake	HadGEM2-ES	469	358	229	243	-9	-10	26	-18
MyLake	IPSL-CM5A-LR	476	376	221	255	-8	-6	21	-14
MyLake	MIROC5	469	382	216	251	-9	-4	19	-15
Simstrat	GFDL-ESM2M	619	487	323	380	20	22	77	28
Simstrat	HadGEM2-ES	632	489	323	387	22	23	77	31
Simstrat	IPSL-CM5A-LR	626	522	391	366	21	31	115	24
Simstrat	MIROC5	599	636	410	374	16	60	125	26
Ensemble mean		577	474	298	321	12	19	64	8
Reference evaporation		517	398	182	296				

Kinneret, demonstrated some differences in the ability of the lake models to capture some of the variability in evaporation rates. This was particularly evident in winter, when seasonal evaporation rates in this lake are at their lowest. However, evaporation rates at this time of year are unlikely to have a considerable influence on annual evaporation rates in this lake, which are the primary focus of our study. Some of the differences between the simulations and reference evaporation are likely due to the meteorological data used to drive the lake models. Specifically, the GCMs used in this study provide historical and future projections of atmospheric conditions at a relatively coarse (0.5°) spatial resolution. The gridded climate data are thus unlikely to capture all of the short-scale spatial variations occurring at the lake surface, particularly given the complex topography in the study region. In addition to these limitations, our model simulations do not consider two-way interactions between the lake and the overlying atmosphere. Furthermore, when evaporation rates are relatively low (e.g., in winter), the percent difference between simulated and reference evaporation will be relatively large.

While we acknowledge the limitations of using GCMs in such regions, these data are undoubtedly the most appropriate to predict future changes in the climate (Busuioc et al., 2001) and, in turn, the studied lake. In an attempt to address the spatial mismatch between observed and simulated meteorological data from the study region, we used bias-corrected GCM output data from ISIMIP2b as input to the lake models (Frieler et al., 2017; Lange, 2019). This bias adjustment essentially alters the statistics of climate simulation data for the purpose of making them more similar to observations. To our knowledge, few studies have used GCM data to project future impacts of climate change on Lake Kinneret (Rimmer et al., 2011), with others using weather generators to forecast changes in the near future (Gal et al., 2020). Finally, the results presented in this study, do not consider ongoing climate change adaptations

carried by the Israeli government. Despite the limitations described above, we believe that our study provides important insights about the future changes in evaporation rates in Lake Kinneret, and is a valuable pilot study for larger scale, across lake, assessments.

The strength of this study is the use of a large ensemble of lake model projections, which has allowed us to identify likely scenarios of future change in lake evaporation within a socioeconomically critical lake. The large ensemble was invaluable in allowing us to not only project future change in evaporation, but also to consider a suite of simulations and, in turn, include uncertainty bounds within our projections. It is our hope that in underscoring the value of including ensemble modelling in lake research, our work motivates continued efforts to employ an ensemble of lake models for better understanding lake responses to climate change. We see good prospects for continued coordination between lake model development, as well as their inclusion in large climate simulations, particularly given the recent expansion of computing resources facilitates including increasing spatial resolution and correspondingly improved process representation (non-thermodynamic processes in lakes, improved large-scale hydrological processes, etc.). We believe that upscaling the multi-model approach introduced in this study to multiple lakes distributed across climatic gradients and in lakes of varying sizes and physiographic characteristics, could provide important insights into lake evaporation variability and responses to climate change.

The access of water resources for human consumption and ecosystem services highly depends on the spatio-temporal distribution of not only evaporation, but also precipitation, two key components of the water budget of lakes (Konapala et al., 2020). In this study, we estimated the impact of changes in both of these metrics, and consequently on P-E, in Lake Kinneret. We found that in all future climate change scenarios, projected changes in lake evaporation were greater than the projected

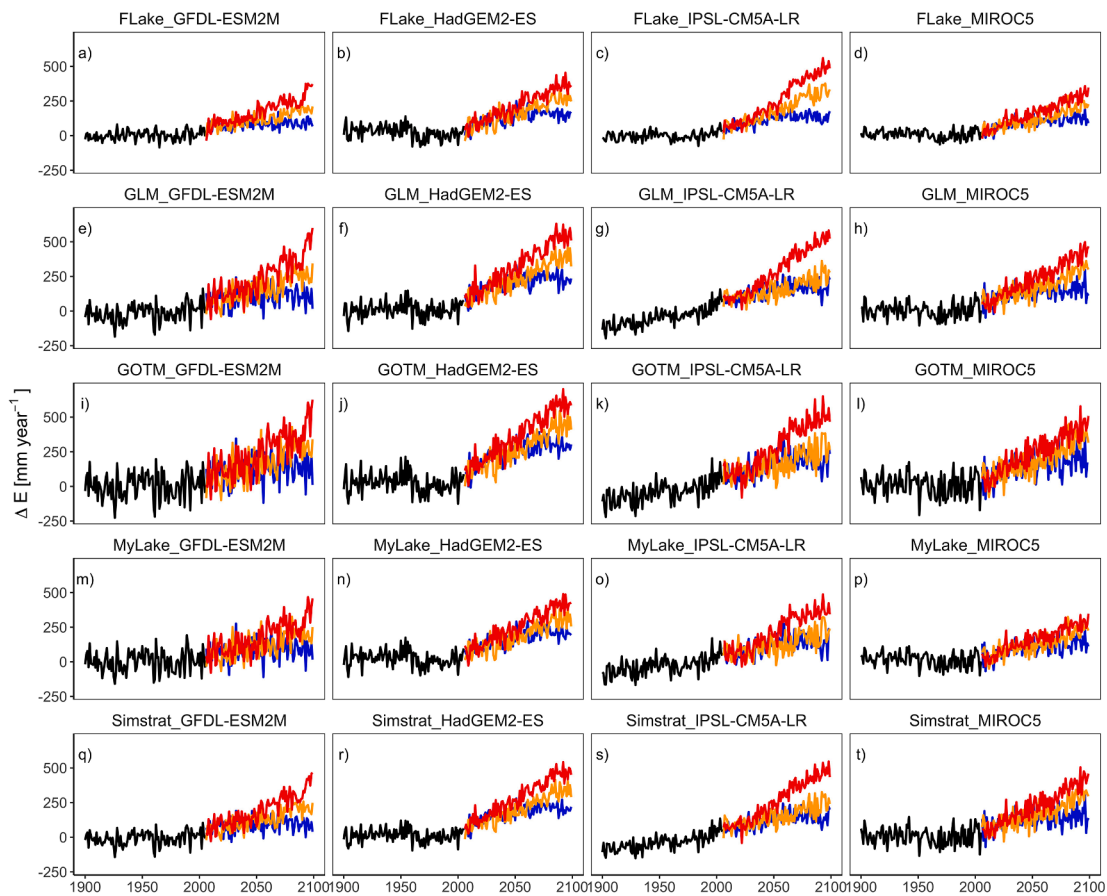


Fig. 5. Projected changes in annual lake evaporation during the historic (1901–2005) and future (2006–2099) periods. Projections are shown for each of the individual lake-climate models, namely for (a–d) FLake, (e–h) GLM, (i–l) GOTM, (m–p) MyLake and (q–t) Simstrat, driven by the four General Circulation Models included in this study. Black lines represent the historical period, and the coloured lines represent the future period, with the blue, orange and red representing the projected change under RCP (Representative Concentration Pathway) 2.6, 6.0, and 8.5, respectively. Anomalies (ΔE) are quoted relative to the 1971–2000 base-period average. (For interpretation of the references to colour in this figure legend, the reader is referred to the web version of this article.)

Table 5

Annual evaporation projections under historical and future scenarios of climate change: RCP 2.6, 6.0 and 8.5 across lake-climate models. The values for the historical period correspond to the average over the 1971–2000 period. The values for the RCP scenarios correspond to the average over the period 2070–2099. Lake evaporation simulations are presented for each lake-climate combination. When presenting the change in evaporation, we also calculate the average for each lake model simulated across the GCMs, shown in bold.

Lake model	Driving GCM	Evaporation [mm year ⁻¹]				Evaporation change [mm year ⁻¹]					
		Historical	RCP 2.6	RCP 6.0	RCP 8.5	RCP 2.6	RCP 6.0	RCP 8.5			
FLake	GFDL-ESM2M	1247	1339	1421	1519	92	127	173	228	272	329
FLake	HadGEM2-ES	1252	1413	1501	1587	160	160	248	248	334	334
FLake	IPSL-CM5A-LR	1257	1393	1555	1698	136	136	298	298	441	441
FLake	MIROC5	1261	1383	1455	1529	121	121	194	194	268	268
GLM	GFDL-ESM2M	2106	2220	2357	2505	114	169	251	278	399	438
GLM	HadGEM2-ES	2110	2351	2469	2609	241	241	359	359	500	500
GLM	IPSL-CM5A-LR	2106	2277	2338	2578	171	171	232	232	472	472
GLM	MIROC5	2118	2269	2386	2500	152	152	268	268	382	382
GOTM	GFDL-ESM2M	2340	2482	2619	2731	141	204	279	313	391	452
GOTM	HadGEM2-ES	2376	2679	2787	2927	303	303	410	410	551	551
GOTM	IPSL-CM5A-LR	2433	2621	2686	2898	187	187	253	253	465	465
GOTM	MIROC5	2597	2782	2909	2998	186	186	312	312	401	401
MyLake	GFDL-ESM2M	1253	1350	1446	1542	96	147	192	220	289	320
MyLake	HadGEM2-ES	1269	1485	1555	1653	216	216	287	287	385	385
MyLake	IPSL-CM5A-LR	1262	1406	1460	1610	145	145	199	199	348	348
MyLake	MIROC5	1277	1406	1480	1535	129	129	203	203	258	258
Simstrat	GFDL-ESM2M	1789	1889	1993	2110	100	153	204	250	321	388
Simstrat	HadGEM2-ES	1805	2020	2116	2240	215	215	311	311	435	435
Simstrat	IPSL-CM5A-LR	1847	1998	2070	2275	151	151	222	222	427	427
Simstrat	MIROC5	1970	2118	2231	2339	148	148	261	261	369	369

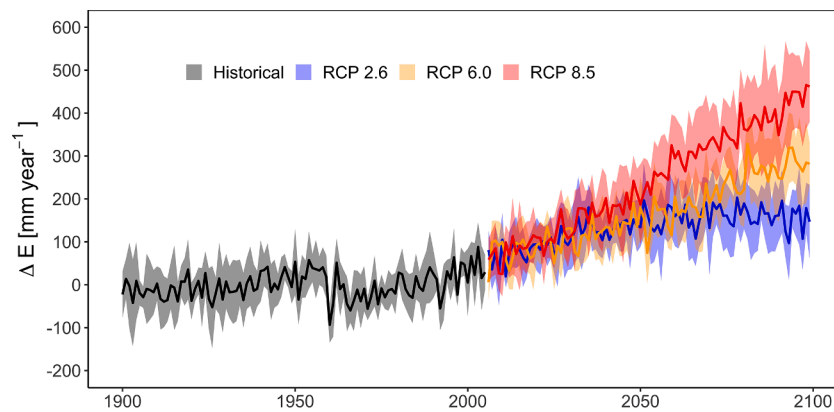


Fig. 6. Projected changes in annual lake evaporation during the historic (1901–2005) and future (2006–2099) periods in Lake Kinneret. The average of the model ensemble is shown by the thick lines, the standard deviation across the model ensemble is represented by the shaded area. Anomalies (ΔE) are quoted relative to the 1971–2000 base period average for RCP (Representative Concentration Pathway) 2.6, 6.0 and 8.5.

Table 6

Annual evaporation projections by the end of the 21st century under future scenarios of climate change: RCP 2.6, 6.0 and 8.5. The evaporation estimates for the historic period correspond to the average over 1971–2000 and the future period corresponds to 2070–2099. Anomalies (Δ) are calculated as future minus historic.

Scenario	Evaporation	Evaporation change (ΔE)	Evaporation change (ΔE)
	[mm year ⁻¹]	[mm year ⁻¹]	[%]
Historical	1784 ± 473	–	–
RCP 2.6	1944 ± 498	160 ± 70	9
RCP 6.0	2042 ± 509	258 ± 76	14
RCP 8.5	2169 ± 530	385 ± 93	22

changes in precipitation, with P-E being predominantly negative, and increasingly so throughout the 21st century. Specifically, by the end of this century, our projections suggest that P-E in Lake Kinneret will decrease by between 14 and 40 % under RCP 2.6 and 8.5, respectively. These projected changes largely align with those described by Givati et al. (2019), who projected a future decrease in precipitation in this region, resulting in a 44 % decrease in the flow of water from the Jordan River (i.e. the main inflow to Lake Kinneret) by 2050–2079 under RCP 8.5. However, similar dramatic changes in the water budget of Lake Kinneret have already been reported, with observational data demonstrating that precipitation in the Kinneret river basin has reduced considerably since 1985 (Givati et al., 2019). Similarly, streamflow observations from the Jordan River indicate that flow rates have decreased by more than 50 % since 2004, provoking historically low

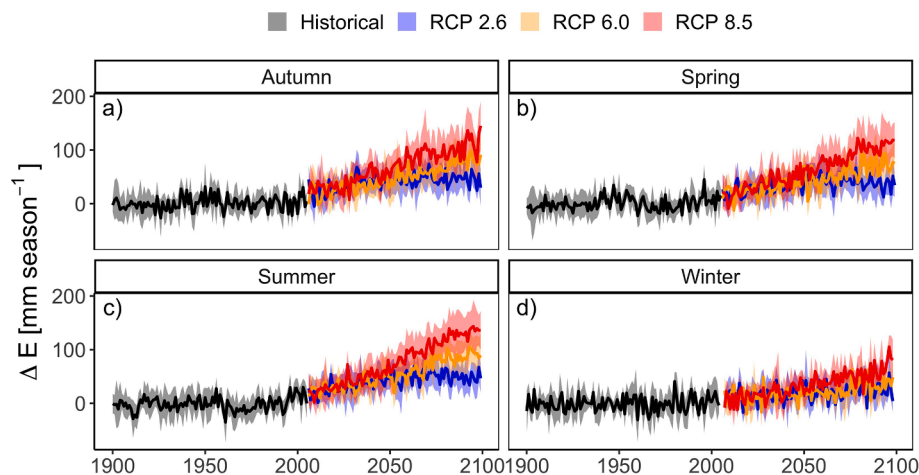


Fig. 7. Projected changes in seasonal lake evaporation during the historic (1901–2005) and future (2006–2099) periods in Lake Kinneret for (a) Autumn, (b) Spring, (c) Summer, and (d) Winter. The average of the model ensemble is shown by the thick lines, the standard deviation across the model ensemble is represented by the shaded area. Anomalies (ΔE) are quoted relative to the 1971–2000 base period average for RCP (Representative Concentration Pathway) 2.6, 6.0 and 8.5.

Table 7

Seasonal evaporation projections by the end of the 21st century under future scenarios of climate change: RCP 2.6, 6.0 and 8.5. The evaporation estimates for the historic period correspond to 1971–2000 and the future estimates correspond to 2070–2099. Anomalies (Δ) are calculated as future minus historic.

Scenarios	Seasonal evaporation change (ΔE) [mm season ⁻¹]				Seasonal evaporation change (ΔE) [%]			
	Autumn	Spring	Summer	Winter	Autumn	Spring	Summer	Winter
	RCP 2.6	46 ± 27	39 ± 27	50 ± 26	24 ± 25	9	12	8
RCP 6.0	72 ± 33	68 ± 32	85 ± 32	32 ± 26	14	20	14	10
RCP 8.5	102 ± 39	101 ± 37	124 ± 36	58 ± 28	20	30	20	19

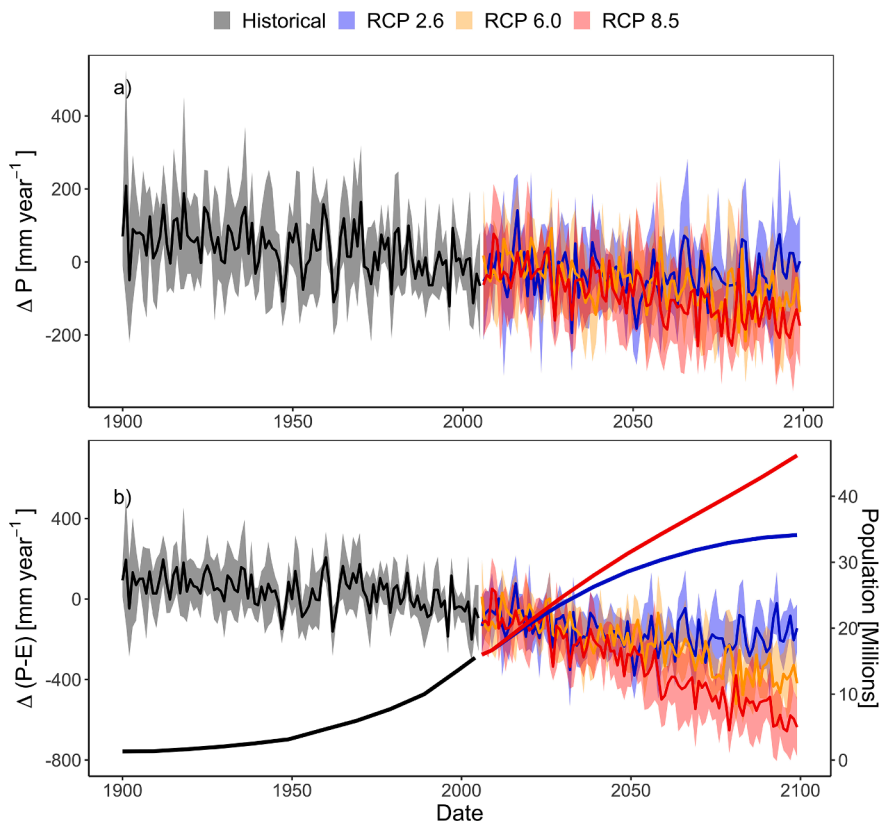


Fig. 8. Projected changes during the historic (1901–2005) and future (2006–2099) periods in Lake Kinneret for (a) precipitation and (b) precipitation minus evaporation (P-E) and population over the study area. The average of the model ensemble is shown by the thick lines and the standard deviation across the model ensemble is represented by the shaded area. Anomalies (ΔP and $\Delta (P-E)$) are quoted relative to the 1971–2000 base period average for RCP (Representative Concentration Pathway) 2.6, 6.0 and 8.5.

Table 8

Summary of precipitation (P), precipitation minus evaporation (P-E), and population changes by the end of the 21st century under future scenarios of climate change: RCP 2.6, 6.0 and 8.5. Estimates for the historic period correspond to 1971–2000 and the future estimates correspond to 2070–2099. Anomalies (Δ) are calculated as future minus historic.

Scenario	ΔP	ΔP	$\Delta (P - E)$	$\Delta (P - E)$	Population	Population change
	[mm year ⁻¹]	[%]	[mm year ⁻¹]	[%]	[Million inhabitants]	[%]
Historical	–	–	–	–	10	–
RCP 2.6	-28 ± 109	–6	-188 ± 129	–14	33	248
RCP 6.0	-98 ± 117	–22	-356 ± 148	–27	(*)	(*)
RCP 8.5	-145 ± 102	–32	-530 ± 145	–40	42	337

(*) Data not available.

levels in Lake Kinneret in 2018 (Tal, 2019).

If the P-E balance of Lake Kinneret changes in-line with our future projections, water availability in the region will likely be severely stressed this century. Notably, in the absence of substantial water inflow changes (e.g., less water extraction for irrigation), a decrease in P-E will likely reduce the total lake volume (Zhou et al., 2021). Our analysis has also demonstrated that a decline in P-E this century will likely occur in parallel with a rapid growth in population. Most notably, the population in the studied region is projected to increase between 248 % and 337 % by the end of this century under RCP 2.6 and 8.5, respectively. This suggests that a growing population will likely become increasingly dependent on water from Lake Kinneret. Notably, the intensification of water scarcity driven by an increasing deficit in P-E combined with a rapid growth in population, is likely to further enhance the depletion of Lake Kinneret and further enhance the already existing water stress in the region. However, it is also important to note that an increase in water stress within the region might reduce the local population due to possible migration in the future, which is not considered in our assessment. As well as the serious socioeconomic implications of declining water level, influenced by an increasing deficit in P-E, this could lead to critical ecosystem disturbances, such as an increase in salinity with

implications for not only physical lake processes (Ladwig et al., 2021) but also the community composition, biomass, and diversity of phytoplankton, zooplankton, macrophytes and fish (Jeppesen et al., 2015), as well as a weakening of key species, the proliferation of invasive species, and a loss of biodiversity (Zohary and Ostrovsky, 2011).

5. Code availability

The code used to produce the figures in this paper is available from the corresponding author upon request.

Data availability

All lake model simulations, precipitation and population projections are available at <https://data.isimip.org/10.48364/ISIMIP.563533>.

Credit authorship contribution statement

Sofia La Fuente: Conceptualization, Methodology, Validation, Investigation, Writing – original draft, Writing – review & editing, Visualization. **Eleanor Jennings:** Conceptualization, Methodology,

Writing – original draft, Supervision. **Gideon Gal**: Conceptualization, Investigation, Data curation, Writing – review & editing. **Georgiy Kirillin**: Methodology, Formal analysis, Data Curation, Writing – review & editing. **Tom Shatwell**: Methodology, Formal analysis, Data Curation, Writing – review & editing. **Robert Ladwig**: Methodology, Formal analysis, Data Curation, Writing – review & editing. **Tadhg Moore**: Methodology, Formal analysis, Data Curation, Writing – review & editing. **Raoul-Marie Couture**: Methodology, Formal analysis, Data Curation, Writing – review & editing. **Marianne Côté**: Methodology, Formal analysis, Data Curation, Writing – review & editing. **C. Love Råman Vinnå**: Methodology, Formal analysis, Data Curation, Writing – review & editing. **R. Iestyn Woolway**: Conceptualization, Methodology, Writing – original draft, Writing – review & editing, Supervision.

Declaration of Competing Interest

The authors declare that they have no known competing financial interests or personal relationships that could have appeared to influence the work reported in this paper.

Acknowledgments

S.LF was funded by the Irish HEA Landscape programme and DkIT Research Office. R.I.W. was funded by a UKRI Natural Environment Research Council (NERC) Independent Research Fellowship [grant number NE/T011246/1]. We thank the Israel Water Authority, the Israel Hydrological Service and the Kinneret Limnological Laboratory for providing the data observations from Lake Kinneret. For their roles in producing, coordinating, and making available the ISIMIP climate scenarios, we acknowledge the support of the ISIMIP cross sectoral science team. We sincerely appreciate all valuable comments and suggestions from reviewers, which helped us to improve the quality of the manuscript.

Appendix A. Supplementary data

Supplementary data to this article can be found online at <https://doi.org/10.1016/j.jhydrol.2022.128729>.

References

- Amadori, M., Giovannini, L., Toffolon, M., et al., 2021. Multi-scale evaluation of a 3D lake model forced by an atmospheric model against standard monitoring data. *Environ. Modell. Software* 139, 105017. <https://doi.org/10.1016/j.envsoft.2021.105017>.
- Andersen, T.K., Nielsen, A., Jeppesen, E., et al., 2020. Predicting ecosystem state changes in shallow lakes using an aquatic ecosystem model: Lake Hinge, Denmark, an example. *Ecol. Appl.* 30, e02160. <https://doi.org/10.1002/eap.2160>.
- Ayala, A.I., Moras, S., Pierson, D.C., 2020. Simulations of future changes in thermal structure of Lake Erken: proof of concept for ISIMIP2b lake sector local simulation strategy. *Hydrol. Earth Syst. Sci.* 24, 3311–3330. <https://doi.org/10.5194/hess-24-3311-2020>.
- Bärenbold, F., Kipfer, R., Schmid, M., 2022. Dynamic modelling provides new insights into development and maintenance of Lake Kivu's density stratification. *Environ. Modell. Software* 147, 105251. <https://doi.org/10.1016/j.envsoft.2021.105251>.
- Brunke, M.A., Fairall, C.W., Zeng, X., Eymard, L., Curry, J.A., 2003. Which bulk aerodynamic algorithms are least problematic in computing ocean surface turbulent fluxes? *J. Clim.* 16, 619–635. [https://doi.org/10.1175/1520-0442\(2003\)016<0619:WBAAAL>2.0.CO;2](https://doi.org/10.1175/1520-0442(2003)016<0619:WBAAAL>2.0.CO;2).
- Brutsaert, W., 1982. *Evaporation into the atmosphere: Theory, History, and Applications*. D. Reidel.
- Burchard, H., K. Bolding, and M. R. Villarreal. 1999. GOTM, a general ocean turbulence model: theory, implementation and test cases, Space Applications Institute.
- Burchard, H., Bolding, K., Kühn, W., Meister, A., Neumann, T., Umlauf, L., 2006. Description of a flexible and extendable physical–biogeochemical model system for the water column. *Journal of Marine systems* 61, 180–211. <https://doi.org/10.1016/j.jmarsys.2005.04.011>.
- Busuioc, A., Chen, D., Hellström, C., 2001. Performance of statistical downscaling models in GCM validation and regional climate change estimates: application for Swedish precipitation. *Int. J. Climatol.* 21, 557–578. <https://doi.org/10.1002/joc.624>.
- Enstad, L.I., Rygg, K., Haugan, P.M., Alendal, G., 2008. Dissolution of a CO₂ lake, modeled by using an advanced vertical turbulence mixing scheme. *Int. J. Greenhouse Gas Control* 2, 511–519. <https://doi.org/10.1016/j.ijggc.2008.04.001>.
- Fairall, C.W., Bradley, E.F., Rogers, D.P., Edson, J.B., Young, G.S., 1996. Bulk parameterization of air-sea fluxes for tropical ocean-global atmosphere coupled-ocean atmosphere response experiment. *J. Geophys. Res. Oceans* 101, 3747–3764. <https://doi.org/10.1029/95JC03205>.
- Fairall, C.W., Bradley, E.F., Hare, J., Grachev, A.A., Edson, J.B., 2003. Bulk parameterization of air-sea fluxes: updates and verification for the COARE algorithm. *J. Clim.* 16, 571–591. [https://doi.org/10.1175/1520-0442\(2003\)016<0571:BPOASF>2.0.CO;2](https://doi.org/10.1175/1520-0442(2003)016<0571:BPOASF>2.0.CO;2).
- Feldbauer, J., Ladwig, R., Mesman, J., Moore, T., Zündorf, H., Berendonk, T.U., Petzoldt, T., 2022. Ensemble of models shows coherent response of a reservoir's stratification and ice cover to climate warming. *Aquat. Sci.* 84, 50. <https://doi.org/10.1007/s00027-022-00883-2>.
- Friedrich, K., Grossman, R.L., Huntington, J., et al., 2018. Reservoir evaporation in the Western United States: current science, challenges, and future needs. *Bull. Am. Meteorol. Soc.* 99, 167–187. <https://doi.org/10.1175/BAMS-D-15-00224.1>.
- Frieler, K., Lange, S., Piontek, F., et al., 2017. Assessing the impacts of 1.5 C global warming–simulation protocol of the Inter-Sectoral Impact Model Intercomparison Project (ISIMIP2b). *Geosci. Model Dev.* <https://doi.org/10.5194/gmd-10-4321-2017>.
- Gal, G., Yael, G., Noam, S., Moshe, E., Schlabing, D., 2020. Ensemble modeling of the impact of climate warming and increased frequency of extreme climatic events on the thermal characteristics of a Sub-Tropical Lake. *Water* 12, 1982. <https://doi.org/10.3390/w12071982>.
- Gal, G., Imberger, J., Zohary, T., Antenucci, J., Anis, A., Rosenberg, T., 2003. Simulating the thermal dynamics of Lake Kinneret. *Ecol. Model.* 162, 69–86. [https://doi.org/10.1016/S0304-3800\(02\)00380-0](https://doi.org/10.1016/S0304-3800(02)00380-0).
- Gaudard, A., Råman Vinnå, L., Bärenbold, F., Schmid, M., Bouffard, D., 2019. Toward an open access to high-frequency lake modelling and statistics data for scientists and practitioners—the case of Swiss lakes using Simstrat v2. 1. *Geosci. Model Dev.* 12, 3955–3974. <https://doi.org/10.5194/gmd-12-3955-2019>.
- Givati, A., Thirel, G., Rosenfeld, D., Paz, D., 2019. Climate change impacts on streamflow at the upper Jordan river based on an ensemble of regional climate models. *J. Hydrol.: Reg. Stud.* 21, 92–109. <https://doi.org/10.1016/j.ejrh.2018.12.004>.
- Golub, M., Thiery, W., Marcé, R., et al., 2022. A framework for ensemble modelling of climate change impacts on lakes worldwide: the ISIMIP Lake Sector. *Geosci. Model Dev. Discuss.* 1–57. <https://doi.org/10.5194/gmd-2021-433>.
- Goudsmit, G., Burchard, H., Peeters, F., Wüest, A., 2002. Application of k-ε turbulence models to enclosed basins: The role of internal seiches. *J. Geophys. Res. Oceans* 107, 23–31. <https://doi.org/10.1029/2001JC000954>.
- Grant, L., Vanderkelen, I., Gudmundsson, L., et al., 2021. Attribution of global lake systems change to anthropogenic forcing. *Nat. Geosci.* 14, 849–854. <https://doi.org/10.1038/s41561-021-00833-x>.
- Henderson-Sellers, B., 1986. Calculating the surface energy balance for lake and reservoir modelling: a review. *Rev. Geophys.* 24, 625–649. <https://doi.org/10.1029/RG024i003p00625>.
- Hipsey, M. R., L. C. Bruce, C. Boon, and others. 2019. A General Lake Model (GLM 3.0) for linking with high-frequency sensor data from the Global Lake Ecological Observatory Network (GLEON). <https://doi.org/10.5194/gmd-12-473-2019>.
- Hondzo, M., Stefan, H.G., 1993. Lake water temperature simulation model. *J. Hydraul. Eng.* 119, 1251–1273. [https://doi.org/10.1061/\(ASCE\)0733-9429\(1993\)119:11\(1251\)](https://doi.org/10.1061/(ASCE)0733-9429(1993)119:11(1251)).
- Hostetler, S., Bartlein, P., 1990. Simulation of lake evaporation with application to modelling lake level variations of Harney-Malheur Lake, Oregon. *Water Resour. Res.* 26, 2603–2612. <https://doi.org/10.1029/WR026i010p02603>.
- Hostetler, S.W., Bates, G.T., Giorgi, F., 1993. Interactive coupling of a lake thermal model with a regional climate model. *J. Geophys. Res. Atmos.* 98, 5045–5057. <https://doi.org/10.1029/92JD02843>.
- Imberger, J., and J. Patterson. 1981. *A dynamic reservoir simulation model-DYRESM*, 5. 310–361. Academic New York. 542.
- Jeppesen, E., Bruce, S., Naselli-Flores, L., et al., 2015. Ecological impacts of global warming and water abstraction on lakes and reservoirs due to changes in water level and related changes in salinity. *Hydrobiologia* 750, 201–227. <https://doi.org/10.1007/s10750-014-2169-x>.
- Jolliffe, J.K., Kindle, J.C., Shulman, I., Penta, B., Friedrichs, M.A., Helber, R., Arnone, R. A., 2009. Summary diagrams for coupled hydrodynamic-ecosystem model skill assessment. *J. Mar. Syst.* 76, 64–82. <https://doi.org/10.1016/j.jmarsys.2008.05.014>.
- Kirillin, G., 2002. *Modeling of the vertical heat exchange in shallow lakes*. Humboldt-Universität. Doctoral dissertation.
- Kishcha, P., Starobinets, B., Lechinsky, Y., Alpert, P., 2021. Absence of surface water temperature trends in Lake Kinneret despite present atmospheric warming: comparisons with Dead Sea trends. *Rem. Sens.* 13, 3461. <https://doi.org/10.3390/rs13173461>.
- Kiuru, P., Ojala, A., Mammarella, I., Heiskanen, J., Erkkilä, K.-M., Miettinen, H., Vesala, T., Huttala, T., 2019. Applicability and consequences of the integration of alternative models for CO₂ transfer velocity into a process-based lake model. *Biogeosciences* 16, 3297–3317. <https://doi.org/10.5194/bg-16-3297-2019>.
- Kobler, U.G., Schmid, M., 2019. Ensemble modelling of ice cover for a reservoir affected by pumped-storage operation and climate change. *Hydrol. Process.* 33, 2676–2690. <https://doi.org/10.1002/hyp.13519>.
- Konapala, G., Mishra, A.K., Wada, Y., Mann, M.E., 2020. Climate change will affect global water availability through compounding changes in seasonal precipitation and evaporation. *Nat. Commun.* 11, 1–10. <https://doi.org/10.1038/s41467-020-16757-w>.

- Kong, X., Ghaffar, S., Determann, M., et al., 2022. Reservoir water quality deterioration due to deforestation emphasizes the indirect effects of global change. *Water Res.* 118721. <https://doi.org/10.1016/j.watres.2022.118721>.
- Ladwig, R., Rock, L.A., Dugan, H.A., 2021. Impact of salinization on lake stratification and spring mixing. *Limnol. Oceanogr. Lett.* <https://doi.org/10.1002/lo2.10215>.
- Lange, S., 2019. Earth2Observe, WFDEI and ERA-Interim data Merged and Bias-corrected for ISIMIP (EWEMBI), V.1.1, GFZ Data Serv. <https://doi.org/10.5880/pik.2019.004>.
- Laval, B., Imberger, J., Hodges, B.R., Stocker, R., 2003. Modelling circulation in lakes: spatial and temporal variations. *Limnol. Oceanogr.* 48, 983–994. <https://doi.org/10.4319/lo.2003.48.3.0983>.
- Lenters, J., Blanken, P., Healey, N., et al., 2014. Physical controls on lake evaporation across a variety of climates and lake types. In: *Proceedings of the 17th International Workshop on Physical Processes in Natural Waters*, p. 56.
- Lenters, J., J. B. Anderton, P. Blanken, C. Spence, and A. E. Suyker. 2013. Assessing the Impacts of Climate Variability and Change on Great Lakes Evaporation 11. http://glisacimate.org/media/GLISA_Lake_Evaporation.pdf.
- Lenters, J.D., Kratz, T.K., Bowser, C.J., 2005. Effects of climate variability on lake evaporation: Results from a long-term energy budget study of Sparkling Lake, northern Wisconsin (USA). *J. Hydrol.* 308, 168–195. <https://doi.org/10.1016/j.jhydrol.2004.10.028>.
- Li, Y., Li, Z., Ma, N., Zhou, X., Zhang, C., 2013. Lake evaporation: A possible factor affecting lake level changes tested by modern observational data in arid and semi-arid China. *J. Geog. Sci.* 23, 123–135. <https://doi.org/10.1007/s11442-013-0998-6>.
- Likens, G., M. Benbow, T. Burton, E. Van Donk, J. Downing, and R. Gulati. 2009. *Encyclopedia of inland waters*.
- Livingstone, D.M., Imboden, D.M., 1989. Annual heat balance and equilibrium temperature of Lake Aegeri, Switzerland. *Aquat. Sci.* 51, 351–369. <https://doi.org/10.1007/BF00877177>.
- MacIntyre, S., Fram, J.P., Kushner, P.J., Bettez, N.D., W. O'Brien, J. Hobbie, and G. W. Kling., 2009. Climate-related variations in mixing dynamics in an Alaskan arctic lake. *Limnol. Oceanogr.* 54, 2401–2417. https://doi.org/10.4319/lo.2009.54.6_part_2.2401.
- Mahrer, Y., Assouline, S., 1993. Evaporation from Lake Kinneret: 2. Estimation of the Horizontal variability using a two-dimensional numerical mesoscale model. *Water Resour. Res.* 29, 911–916. <https://doi.org/10.1029/92WR02433>.
- Markelov, I., Couture, R., Fischer, R., Haande, S., Van Cappellen, P., 2019. Coupling water column and sediment biogeochemical dynamics: Modeling internal phosphorus loading, climate change responses, and mitigation measures in Lake Vansjø, Norway. *J. Geophys. Res. Biogeosci.* 124, 3847–3866. <https://doi.org/10.1029/2019JG005254>.
- Marsh, P., Bigras, S., 1988. Evaporation from Mackenzie delta lakes, NWT, Canada. *Arct. Alp. Res.* 20, 220–229. <https://doi.org/10.2307/1551500>.
- Mason, L.A., Riseng, C.M., Gronewold, A.D., Rutherford, E.S., Wang, J., Clites, A., Smith, S.D., MacIntyre, P.B., 2016. Fine-scale spatial variation in ice cover and surface temperature trends across the surface of the Laurentian Great Lakes. *Clim. Change* 138, 71–83. <https://doi.org/10.1007/s10584-016-1721-2>.
- McVicar, T.R., Roderick, M.L., Donohue, R.J., et al., 2012. Global review and synthesis of trends in observed terrestrial near-surface wind speeds: implications for evaporation. *J. Hydrol.* 416, 182–205. <https://doi.org/10.1016/j.jhydrol.2011.10.024>.
- Meehl, G.A., Arblaster, J.M., Tebaldi, C., 2005. Understanding future patterns of increased precipitation intensity in climate model simulations. *Geophys. Res. Lett.* 32. <https://doi.org/10.1029/2005GL023680>.
- Mesman, J., Ayala, A.L., Adrian, R., et al., 2020. Performance of one-dimensional hydrodynamic lake models during short-term extreme weather events. *Environ. Modell. Software* 133, 104852. <https://doi.org/10.1016/j.envsoft.2020.104852>.
- Mironov, D. V. 2008. Parameterization of lakes in numerical weather prediction: Description of a lake model, DWD.
- Mishra, V., Cherkauer, K.A., Bowling, L.C., 2011. Changing thermal dynamics of lakes in the Great Lakes region: Role of ice cover feedbacks. *Global Planet. Change* 75, 155–172. <https://doi.org/10.1016/j.gloplacha.2010.11.003>.
- Moore, T.N., Mesman, J.P., Ladwig, R., et al., 2021. LakeEnsemblR: An R package that facilitates ensemble modelling of lakes. *Environ. Modell. Software* 143, 105101. <https://doi.org/10.1016/j.envsoft.2021.105101>.
- Moras, S., Ayala, A.L., Pierson, D.C., 2019. Historical modelling of changes in Lake Erken thermal conditions. *Hydrol. Earth Syst. Sci.* 23, 5001–5016. <https://doi.org/10.5194/hess-23-5001-2019>.
- Pilla, R.M., Couture, R., 2021. Attenuation of photosynthetically active radiation and ultraviolet radiation in response to changing dissolved organic carbon in browning lakes: Modeling and parameterization. *Limnol. Oceanogr.* 66, 2278–2289. <https://doi.org/10.1002/lno.11753>.
- Prange, M., Wilke, T., Wesselingh, F.P., 2020. The other side of sea level change. *Commun. Earth Environ.* 1, 1–4. <https://doi.org/10.1038/s43247-020-00075-6>.
- Råman Vinnå, L., Medhaug, I., Schmid, M., Bouffard, D., 2021. The vulnerability of lakes to climate change along an altitudinal gradient. *Commun. Earth Environ.* 2, 1–10. <https://doi.org/10.1038/s43247-021-00106-w>.
- Read, J.S., Hamilton, D.P., Desai, A.R., et al., 2012. Lake-size dependency of wind shear and convection as controls on gas exchange. *Geophys. Res. Lett.* 39. <https://doi.org/10.1029/2012GL051886>.
- Rimmer, A., Samuels, R., Lechinsky, Y., 2009. A comprehensive study across methods and time scales to estimate surface fluxes from Lake Kinneret, Israel. *J. Hydrol.* 379, 181–192. <https://doi.org/10.1016/j.jhydrol.2009.10.007>.
- Rimmer, A., Givati, A., Samuels, R., Alpert, P., 2011. Using ensemble of climate models to evaluate future water and solutes budgets in Lake Kinneret, Israel. *J. Hydrol.* 410, 248–259. <https://doi.org/10.1016/j.jhydrol.2011.09.025>.
- Riveros-Iregui, D.A., Lenters, J.D., Peake, C.S., Ong, J.B., Healey, N.C., Zlotnik, V.A., 2017. Evaporation from a shallow, saline lake in the Nebraska Sandhills: energy balance drivers of seasonal and interannual variability. *J. Hydrol.* 553, 172–187. <https://doi.org/10.1016/j.jhydrol.2017.08.002>.
- Sachse, R., Petzoldt, T., Blumstock, M., et al., 2014. Extending one-dimensional models for deep lakes to simulate the impact of submerged macrophytes on water quality. *Environ. Modell. Software* 61, 410–423. <https://doi.org/10.1016/j.envsoft.2014.05.023>.
- Salk, K.R., Venkiteswaran, J.J., Couture, R., Higgins, S.N., Paterson, M.J., Schiff, S.L., 2022. Warming combined with experimental eutrophication intensifies lake phytoplankton blooms. *Limnol. Oceanogr.* 67, 147–158. <https://doi.org/10.1002/lno.11982>.
- Saloranta, T.M., Andersen, T., 2007. MyLake—A multi-year lake simulation model code suitable for uncertainty and sensitivity analysis simulations. *Ecol. Model.* 207, 45–60. <https://doi.org/10.1016/j.ecolmodel.2007.03.018>.
- Schindler, D.W., 2001. The cumulative effects of climate warming and other human stresses on Canadian freshwaters in the new millennium. *Can. J. Fish. Aquat. Sci.* 58, 18–29. https://doi.org/10.1007/978-1-4615-1493-0_11.
- Shilo, E., Ziv, B., Shamir, E., Rimmer, A., 2015. Evaporation from Lake Kinneret, Israel, during hot summer days. *J. Hydrol.* 528, 264–275. <https://doi.org/10.1016/j.jhydrol.2015.06.042>.
- Spence, C., Blanken, P., Lenters, J.D., Hedstrom, N., 2013. The importance of spring and autumn atmospheric conditions for the evaporation regime of Lake Superior. *J. Hydrometeorol.* 14, 1647–1658. <https://doi.org/10.1175/JHM-D-12-0170.1>.
- Tal, A., 2019. Climate change's impact on Lake Kinneret: letting the data tell the story. *Sci. Total Environ.* 685, 1272–1275. <https://doi.org/10.1016/j.scitotenv.2019.05.282>.
- Thiery, W., Stepanenko, V.M., Fang, X., et al., 2014. LakeMIP Kivu: evaluating the representation of a large, deep tropical lake by a set of one-dimensional lake models. *Tellus A: Dynamic Meteorology and Oceanography* 66, 21390. <https://doi.org/10.3402/tellusa.v66.21390>.
- Trolle, D., Elliott, J.A., Mooij, W.M., Janse, J.H., Bolding, K., Hamilton, D.P., Jeppesen, E., 2014. Advancing projections of phytoplankton responses to climate change through ensemble modelling. *Environ. Modell. Software* 61, 371–379. <https://doi.org/10.1016/j.envsoft.2014.01.032>.
- Umlauf, L., Lemmin, U., 2005. Interbasin exchange and mixing in the hypolimnion of a large lake: the role of long internal waves. *Limnol. Oceanogr.* 50, 1601–1611. <https://doi.org/10.4319/lo.2005.50.5.1601>.
- Vallet-Coulomb, C., Legesse, D., Gasse, F., Travi, Y., Chernet, T., 2001. Lake evaporation estimates in tropical Africa (lake Ziway, Ethiopia). *J. Hydrol.* 245, 1–18. [https://doi.org/10.1016/S0022-1694\(01\)00341-9](https://doi.org/10.1016/S0022-1694(01)00341-9).
- Van Cleave, K., Lenters, J.D., Wang, J., Verhamme, E.M., 2014. A regime shift in Lake Superior ice cover, evaporation, and water temperature following the warm El Niño winter of 1997–1998. *Limnol. Oceanogr.* 59, 1889–1898. <https://doi.org/10.4319/lo.2014.59.6.1889>.
- Van Emmerik, T., Rimmer, A., Lechinsky, Y., Wenker, K., Nussboim, S., Van de Giesen, N., 2013. Measuring heat balance residual at lake surface using Distributed Temperature Sensing. *Limnol. Oceanogr. Methods* 11, 79–90. <https://doi.org/10.4319/lom.2013.11.79>.
- Verburg, P., Antenucci, J.P., 2010. Persistent unstable atmospheric boundary layer enhances sensible and latent heat loss in a tropical great lake: Lake Tanganyika. *J. Geophys. Res.: Atmos.* 115. <https://doi.org/10.1029/2009JD012839>.
- Wahed, M.S.A., Mohamed, E.A., El-Sayed, M.I., Mnif, A., Sillanpää, M., 2014. Geochemical modelling of evaporation process in Lake Qarun, Egypt. *J. Afr. Earth Sci.* 97, 322–330. <https://doi.org/10.1016/j.jafrearsci.2014.05.008>.
- Wang, W., Lee, X., Xiao, W., Liu, S., Schultz, N., Wang, Y., Zhang, M., Zhao, L., 2018. Global lake evaporation accelerated by changes in surface energy allocation in a warmer climate. *Nature Geosci.* 11, 410–414. <https://doi.org/10.1038/s41561-018-0114-8>.
- Williamson, C.E., Saros, J.E., Vincent, W.F., Smol, J.P., 2009. Lakes and reservoirs as sentinels, integrators, and regulators of climate change. *Limnol. Oceanogr.* 54, 2273–2282. https://doi.org/10.4319/lo.2009.54.6_part_2.2273.
- Winslow, L.A., Zwart, J.A., Batt, R.D., Dugan, H.A., Woolway, R.I., Corman, J.R., Hanson, P.C., Read, J.S., 2016. LakeMetabolizer: an R package for estimating lake metabolism from free-water oxygen using diverse statistical models. *Inland Waters* 6, 622–636. <https://doi.org/10.1080/IW-6.4.883>.
- Woolway, R.I., Merchant, C.J., 2018. Intralake heterogeneity of thermal responses to climate change: a study of large northern hemisphere lakes. *J. Geophys. Res.: Atmos.* 123, 3087–3098. <https://doi.org/10.1002/2017JD027661>.
- Woolway, R.I., Jones, I.D., Hamilton, D.P., Maberly, S.C., Muraoka, K., Read, J.S., Smyth, R.L., Winslow, L.A., 2015. Automated calculation of surface energy fluxes with high-frequency lake buoy data. *Environ. Modell. Software* 70, 191–198. <https://doi.org/10.1016/j.envsoft.2015.04.013>.
- Woolway, R.I., Verburg, P., Lenters, J.D., et al., 2018. Geographic and temporal variations in turbulent heat loss from lakes: a global analysis across 45 lakes. *Limnol. Oceanogr.* 63, 2436–2449. <https://doi.org/10.1002/lno.10950>.
- Woolway, R.I., Kraemer, B.M., Lenters, J.D., Merchant, C.J., O'Reilly, C.M., Sharma, S., 2020. Global lake responses to climate change. *Nature Rev. Earth Environ.* 1–16. <https://doi.org/10.1038/s43017-020-0067-5>.
- Woolway, R.I., Sharma, S., Weyhenmeyer, G.A., et al., 2021. Phenological shifts in lake stratification under climate change. *Nat. Commun.* 12, 1–11. <https://doi.org/10.1038/s41467-021-22657-4>.
- Ye, X., Anderson, E.J., Chu, P.Y., Huang, C., Xue, P., 2019. Impact of water mixing and ice formation on the warming of Lake Superior: a model-guided mechanism study. *Limnol. Oceanogr.* 64, 558–574. <https://doi.org/10.1002/lno.11059>.
- Zamani, B., Koch, M., Hodges, B.R., 2021. A potential tipping point in the thermal regime of a warm monomictic reservoir under climate change using three-dimensional hydrodynamic modelling. *Inland Waters* 11, 315–334.

- Zeng, X., Zhao, M., Dickinson, R.E., 1998. Intercomparison of bulk aerodynamic algorithms for the computation of sea surface fluxes using TOGA COARE and TAO data. *J. Clim.* 11, 2628–2644.
- Zhan, S., Song, C., Wang, J., Sheng, Y., Quan, J., 2019. A global assessment of terrestrial evapotranspiration increase due to surface water area change. *Earth's Future* 7, 266–282. <https://doi.org/10.1029/2018EF001066>.
- Zhou, W., Wang, L., Li, D., Leung, L.R., 2021. Spatial pattern of lake evaporation increases under global warming linked to regional hydroclimate change. *Commun. Earth Environ.* 2, 1–10. <https://doi.org/10.1038/s43247-021-00327-z>.
- Zohary, T., Ostrovsky, I., 2011. Ecological impacts of excessive water level fluctuations in stratified freshwater lakes. *Inland Waters* 1, 47–59. <https://doi.org/10.5268/IW-1.1.406>.
- Zohary, T., Sukenik, A., Berman, T., Nishri, A., 2014. *Lake Kinneret: Ecology and Management*. Springer.